Heliyon 10 (2024) e35727

Contents lists available at ScienceDirect

Heliyon

journal homepage: www.cell.com/heliyon

Research article

Exosomal CTHRC1 from cancer-associated fibroblasts facilitates endometrial cancer progression via ITGB3/FAK signaling pathway

Yiding Bian [a,1], Xinwen Chang [b,1], Xiang Hu [a], Bilan Li [a], Yunfeng Song [a], Zhiyi Hu [c], Kai Wang [c,*], Xiaoping Wan [a,**], Wen Lu [a,***]

[a] Department of Gynecology, Shanghai First Maternity and Infant Hospital, Tongji University School of Medicine, Shanghai, China
[b] Department of Assisted Reproductive Medicine, Shanghai First Maternity and Infant Hospital, Tongji University School of Medicine, Shanghai, China
[c] Clinical and Translational Research Centre, Shanghai First Maternity and Infant Hospital, Tongji University School of Medicine, Shanghai, China

ARTICLE INFO

Keywords:
Endometrial cancer
Exosome
CAF
CTHRC1
Metastatic

ABSTRACT

The emerging tumor microenvironment (TME) is a complex and constantly evolving entity. Cancer-associated fibroblasts (CAFs) are a vital component of the TME with diverse functions. They interact closely with cancer cells through reciprocal signaling and play a crucial role in tumor progression. Exosomes, which contain diverse biological information, are identified as an important mediator of cell–cell communication. This study aimed to investigate how CAF-derived exosomes promote metastasis of endometrial cancer (EC). Our findings revealed that CAF-derived exosomes significantly enhanced EC cell proliferation and migration compared to normal fibroblast-derived exosomes. Quantitative proteomics analysis of CAF/NF-derived exosomes demonstrated differential expression of CTHRC1, a protein overexpressed in multiple tumors, promoting cancer progression through enhanced cell migration and invasion. Exosomal overload of CTHRC1 significantly contributes to EC cell migration. Mechanically, we determined that ITGB3 was immunoprecipitated by CTHRC1 and phosphorylated FAK on Tyr397, which was important for exosomal CTHRC1 mediated migratory ability of EC cells. Overexpression of CTHRC1 in secreted exosomes promotes the metastatic ability of EC cells in mouse models and may be eliminated by Defactinib, an inhibitor of FAK Tyr397 phosphorylation. Moreover, overexpression of CTHRC1 was increased in EC patients, elevating with cancer progression, and correlated with negative tumor prognosis. Our results revealed that CAF mediated endometrial cancer progression is related to high levels of CTHRC1 and exosomal CTHRC1 derived from CAF may be a promising therapeutic strategy for metastatic endometrial cancer.

1. Introduction

Endometrial cancer (EC) is the sixth most common cancer among females, with 417,000 new cases recorded worldwide in 2020 [1].

* Corresponding author.
** Corresponding author.
*** Corresponding author. Shanghai First Maternity and Infant Hospital, Tongji University School of Medicine, 2699 West Gaoke Road, Pudong, Shanghai, 200040, China.
E-mail addresses: kaiwangcn@yahoo.com (K. Wang), xiaopingwan33@163.com (X. Wan), dr_luwen@tongji.edu.cn (W. Lu).
[1] These authors contributed equally.

https://doi.org/10.1016/j.heliyon.2024.e35727
Received 15 April 2024; Received in revised form 24 July 2024; Accepted 2 August 2024
Available online 6 August 2024

Although the majority of patients diagnosed have early-stage disease with a good prognosis after surgery alone, adjuvant therapy options for this cancer remain intricate and controversial, with few therapeutic alternatives available for metastatic disease [2,3]. Therefore, it is crucial to gain a comprehensive understanding of the molecular mechanisms underlying the development, metastasis, and recurrence of endometrial cancer, in order to develop targeted treatment strategies to impede tumor progression, ultimately enhancing survival rates of patients with high-grade endometrial cancer.

Previous research on the pathogenesis and progression of endometrial cancer has predominantly focused on aberrant activation of intracellular signaling pathways resulting from genetic mutations within tumor cells. However, challenges have emerged with conventional chemo, radiation, and targeted therapies aimed at targeting distinctive signaling pathways activated by genetic mutations in tumor cells. The constantly evolving knowledge about the complexity of the cancer niche and the dynamic interactions between all its components has changed the way we think about tumors [4]. The highly complex and heterogenous ecosystem of a tumour not only contains malignant cells, but also interacting cells from the host such as endothelial cells, stromal fibroblasts, and diverse immune cells regulating tumour growth and invasion [5,6].

The past few years have witnessed a great expansion in research related to cancer-associated fibroblasts (CAFs). As a key component of the TME, CAFs play a role in shaping the TME in four main ways: tumor proliferation and metastasis, angiogenesis, ECM remodeling, and immunosuppression [7]. CAFs derived from EC tissues promoted EC progression via releasing IL-6, transforming growth factor-β (TGF-β) and stromal cell derived factor-1 (SDF-1α) a paracrine- or autocrine-dependent mode [8–10]. CAFs are capable of secreting a variety of matrix metalloproteinases (MMPs), modifying the ECM, and facilitating tumor progression and metastasis [11]. Suppressed expression of miR-148a in CAFs promotes the migration of endometrial cancer cells by targeting Wnt10B to activate

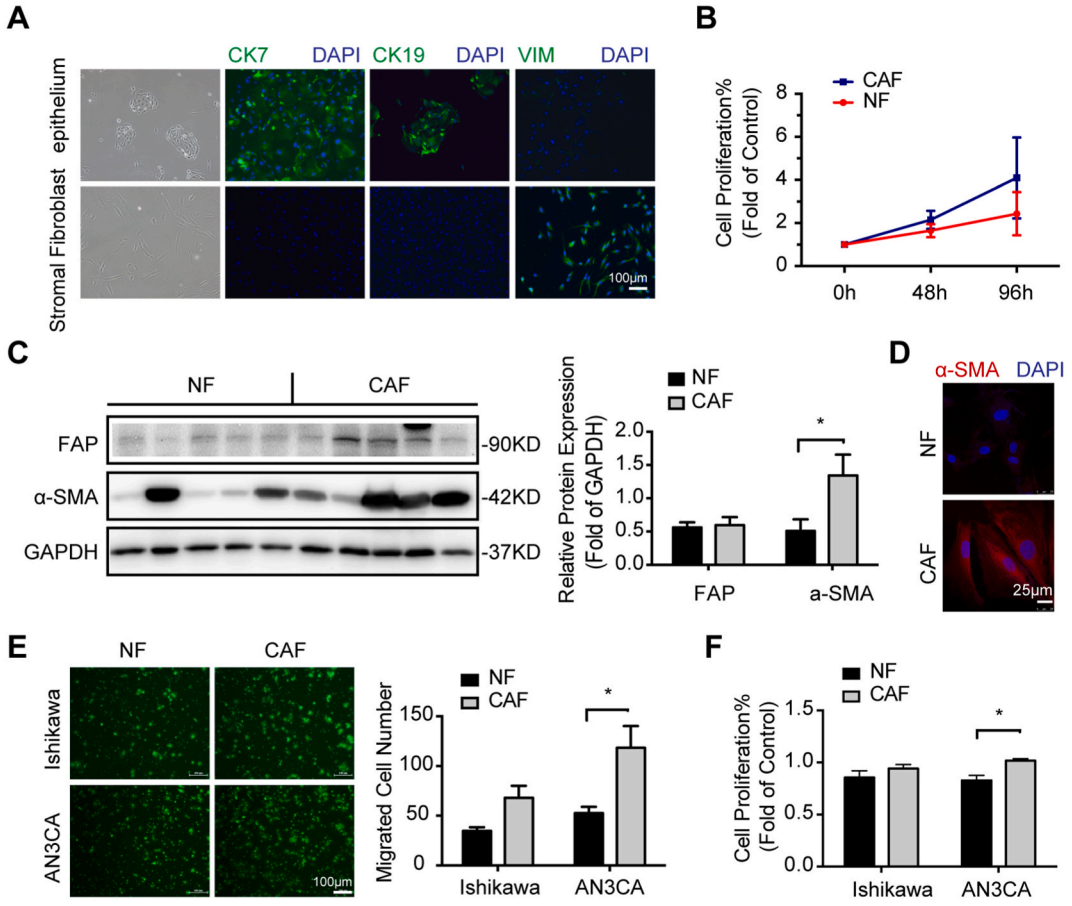

Fig. 1. Characterization of primary NFs and CAFs. A Cell morphology (Left, 40×) and biomarkers (CK7 and CK9 for epithelial cells, green; Vimentin for stromal fibroblasts, green) of primary endometrial epithelial cells and stromal fibroblasts; DAPI in blue; Scale bar: 100 μm. B Cell proliferation of primary normal fibroblasts (NFs) and cancer-associated fibroblasts (CAFs) (n = 5). C Western blot analysis of the protein level of activated fibroblasts markers, FAP and α-SMA (n = 5 for NFs and n = 5 for CAFs; *P < 0.05). Expression of GAPDH was used as internal control. D Expression and localization of α-SMA (red) using immunofluorescence; DAPI in blue. E Cell migration capabilities of EC cells (Ishikawa and AN3CA) in response to co-culturing with NFs and CAFs for 48 h (scale bar: 100 μm; *P < 0.05). F After co-culturing with NFs and CAFs for 48 h, EC cell proliferation were measured by cell counting kit-8 assays (*$P < 0.05$).

All data shown are represented as the means ± SEMs of three pairs of independent experiments. (For interpretation of the references to colour in this figure legend, the reader is referred to the Web version of this article.)

the Wnt/β-catenin pathway [12]. Compared to normal fibroblasts (NF) in the endometrium, CAFs exhibited decreased levels of cell-surface poliovirus receptor (PVR/CD155), a ligand of activating NK receptor DNAM-1, leading to suppression of NK cell activity [13]. Taken together, intercellular communication plays a critical role in tumor progression and metastasis, and CAFs promote the progression of EC with diverse functions.

Exosomes are cell secreted, between 30 and 150 nm thick, consisting of a lipid bilayer membrane that shields them from proteases and RNases and is widely distributed in different biological or bodily fluids [14,15]. Increasing evidence indicates that these vesicles shuttle biological components such as microRNAs, long non-coding RNAs, DNA, and proteins to recipient cells, playing key roles in different physiological processes [16–18]. However, the potential roles of exosomes originating from CAFs in the EC remain uncertain.

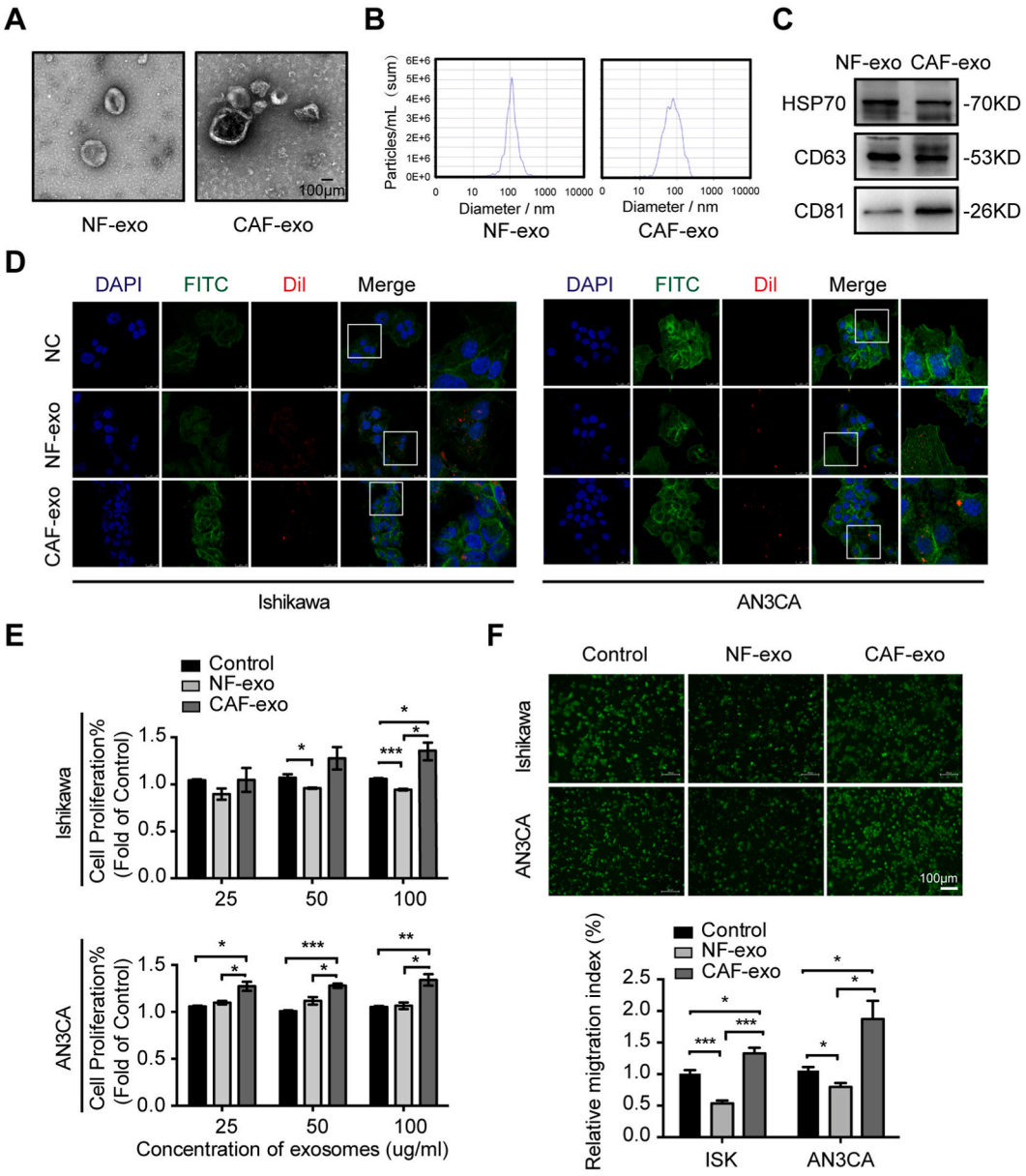

Fig. 2. CAF-derived Exosomes Increased Proliferation and Migration of EC Cells *in vitro* A Isolated exosomes were examined for morphology and size via transmission electron microscopy (scale bar: 100 nm) B Nanoparticle tracking analysis (NTA) profile of exosomes derived from NFs (left) and CAFs (right). C Western blot analysis of exosomal marker expression (HSP70, CD63, CD81). D Ishikawa and AN3CA cells were incubated with 1,10-dioctadecyl-3,3,30,30-tetra- methylindocarbocyanine perchlorate (Dil)-labeled exosomes (100 μg/ml) or negative controls for 16 h (Dil in red, phalloidin-FITC in green, and DAPI in blue). E After incubation with exosomes (25, 50, 100 μg/ml) for 72 h, the proliferation of Ishikawa and AN3CA cells were measured by cell counting kit-8 assay (n = 5 per group; *P < 0.05; ***P < 0.001) F Migration of EC cells in response to exosomes (100 μg/ml) was determined; scale bar: 100 μm (n = 5 per group; *$P < 0.05$; ***$P < 0.001$). (For interpretation of the references to colour in this figure legend, the reader is referred to the Web version of this article.)

In the present study, we found that CAF-derived exosomes were capable of promoting EC cell migration. By analyzing proteins present in exosomes from CAFs and normal fibroblasts (NFs), we identified elevated levels of Collagen triple helix repeat containing-1 (CTHRC1) in CAFs. Importantly, exosomal CTHRC1 facilitated EC progression by regulating the ITGB3/FAK pathway in target EC cells. Overall, our findings uncover a novel network mediated by exosomal CTHRC1 during EC progression, highlighting the potential of targeting the TME for therapeutic strategies against EC.

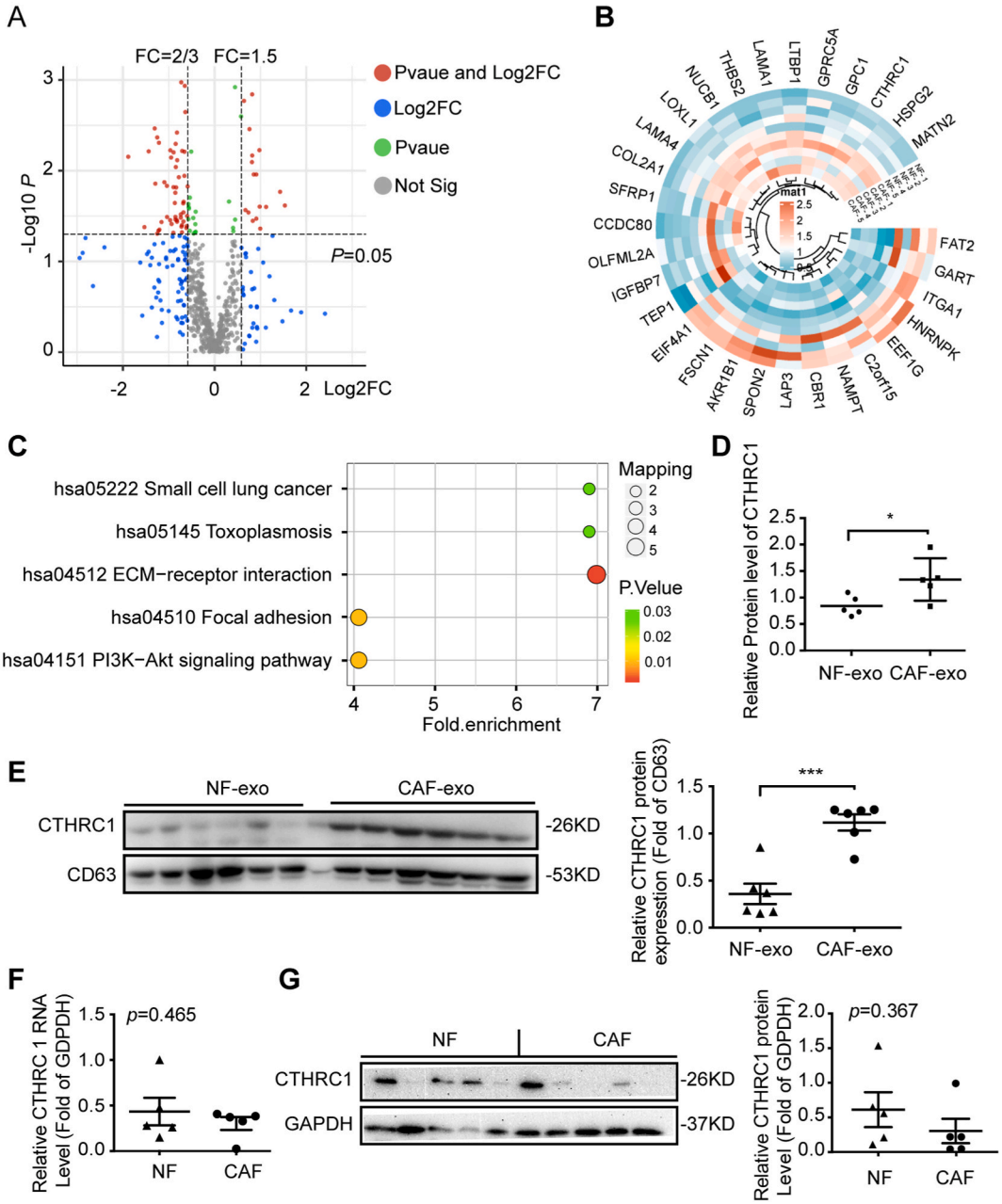

Fig. 3. Identification of Oncogenic Protein CTHRC1 in CAF-derived exosomes A The volcanogram of differential proteins for NF-exo vs CAF exo. The data are shown as x (Log2FC)-y (Log10 p value) scatter plots. FC value > 1.5 or <2/3 and P value < 0.05 were set as the filter criteria. Red dots represent significant upregulated or downregulated proteins. B Heatmap of differentially expressed proteins (FC values > 1.5 or <0.5 and P value < 0.05). C KEGG pathway enrichment analysis was performed on proteins expressed differently. The top 5 items are listed based on their statistical significance. D CTHRC1 levels of exosomes according to proteomic analysis (n = 5, *P < 0.05) E Western blot analysis confirmed CTHRC1 levels were elevated in CAF-exo (n = 6 in each group, ***P < 0.001, with CD63 as the control)

F,G RNA and protein levels of CTHRC in NFs and CAFs. (For interpretation of the references to colour in this figure legend, the reader is referred to the Web version of this article.)

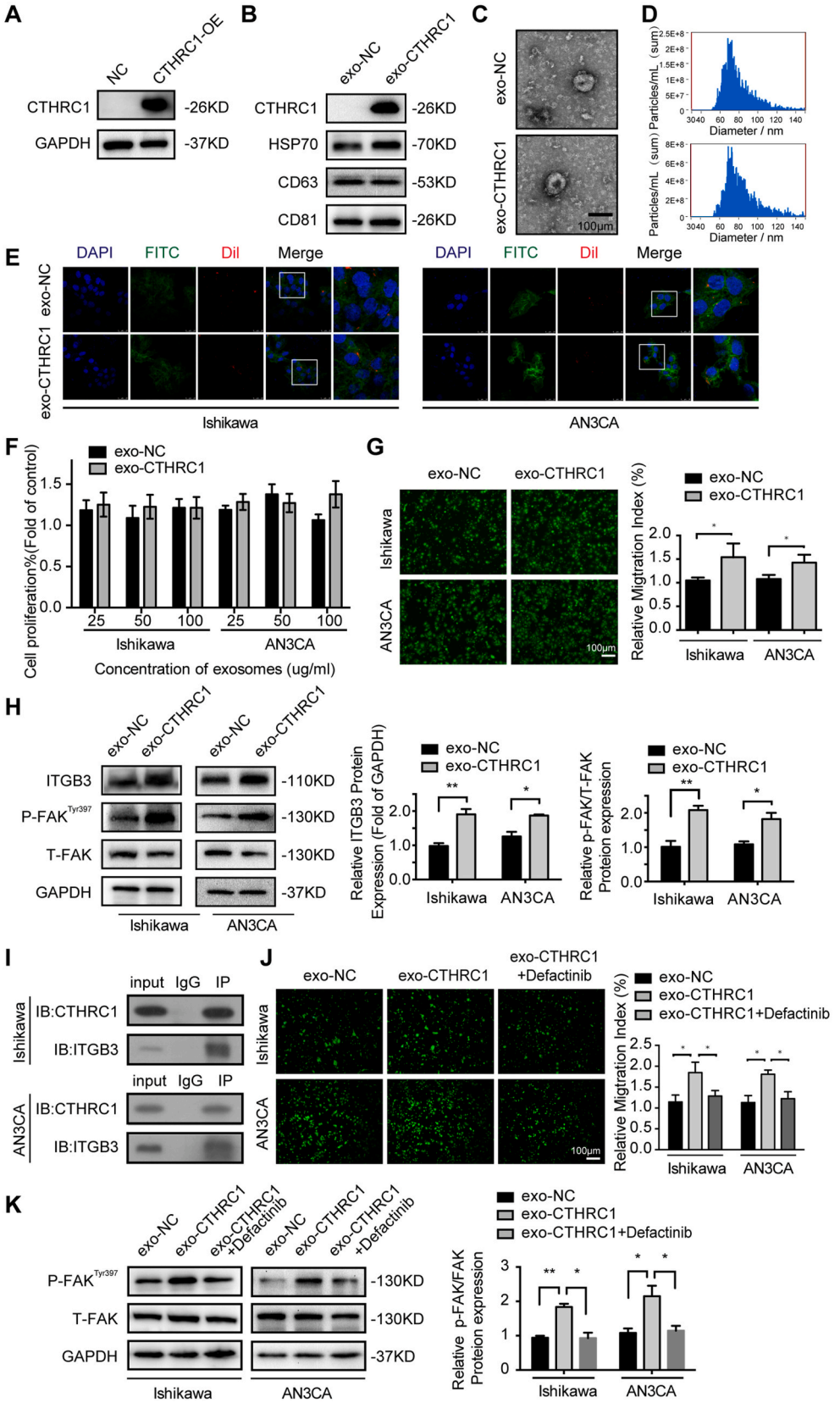

(caption on next page)

Fig. 4. Abundant CTHRC1-loaded exosomes contribute EC cell migration via the activation of the ITGB3/FAK signaling pathway A Western blot analysis of CTHRC1 in HEK293 cells, transfected with lentiviral vectors to stable overexpress CTHRC1, empty lentivirus was used as negative control. **B** The presence of exosomal CTHRC1 and exosomal markers HSP70, CD63, and CD81 was detected by Western blotting. **C,D** The morphology and vesicle size distribution of exo-NC and exo-CTHRC1 were observed by TEM and NTA (TEM scale bar: 100 nm). **E** Exosomes (exo-NC, exo-CTHRC1) labeled with 1,10-dioctadecyl-3,3,30,30-tetramethylindocarbocyanine perchlorate (Dil, red) were taken up by Ishikawa and AN3CA cells (phalloidin-FITC in green, DAPI in blue), with PBS as negative control. **F** Cell proliferation following treatment with exo-CTHRC1 (25, 50 and 100 μg/ml) for 72 h as compared to exo-NC treatment were measured by cell counting kit-8 assays. **G** Cell migration of Ishikawa and AN3CA cells in response to exosomes (exo-NC, exo-CTHRC1,100 μg/ml) was assessed; scale bar: 100 μm (*$p < 0.05$). **H** The protein levels of ITGB3, *p*-FAK (Tyr397) and FAK after exo-CTHRC1 treatment (100 μg/ml) in EC cells were evaluated by Western blotting (GAPHD was used for normalization). I CTHRC1 was immunoprecipitated with ITGB3 antibody in Ishikawa and AN3CA cells after incubation with CTHRC1-enriched exosomes for 16 h. **J, K** EC cells were treated with exo-NC, exo-CTHRC1 and exo-CTHRC1+ Defactinib (inhibitor of FAK Tyr397 phosphorylation) for 16 h. Defactinib inhibited exosomal CTHRC1-induced phosphorylation of FAK (Tyr397) and cell migration in Ishikawa and AN3CA cells (*$P < 0.05$). (For interpretation of the references to colour in this figure legend, the reader is referred to the Web version of this article.)

2. Results

2.1. Characterization of primary NFs and CAFs

Stromal fibroblasts were isolated from normal endometrium (n = 5) and EC tissue (n = 5). As shown in Fig. 1A, stromal fibroblasts had an elongated mesenchymal morphology, expressed a high level of Vimentin, and virtually no CK7 and CK19. In contrast, primary endometrial epithelial cells grew in cluster configurations and were positively stained by CK7 and CK19, which were considered markers of epithelial cells. The growth capacity of CAFs showed an increasing trend compared to NFs, but the comparison result was not statistically significant (Fig. 1B). Moreover, CAFs expressed higher α-SMA than NFs, whereas there is no statistical significance in differential AFP expression (Fig. 1C and D). Considering the important role of cell extrinsic factors on cell growth and migration, a cell coculture system was used to investigate the intercellular interaction between NFs/CAFs and endometrial cancer cells. Cocultured with CAFs for 48 h could enhance cell proliferation and migration capabilities of AN3CA cells, compared to NFs (Fig. 1E and F).

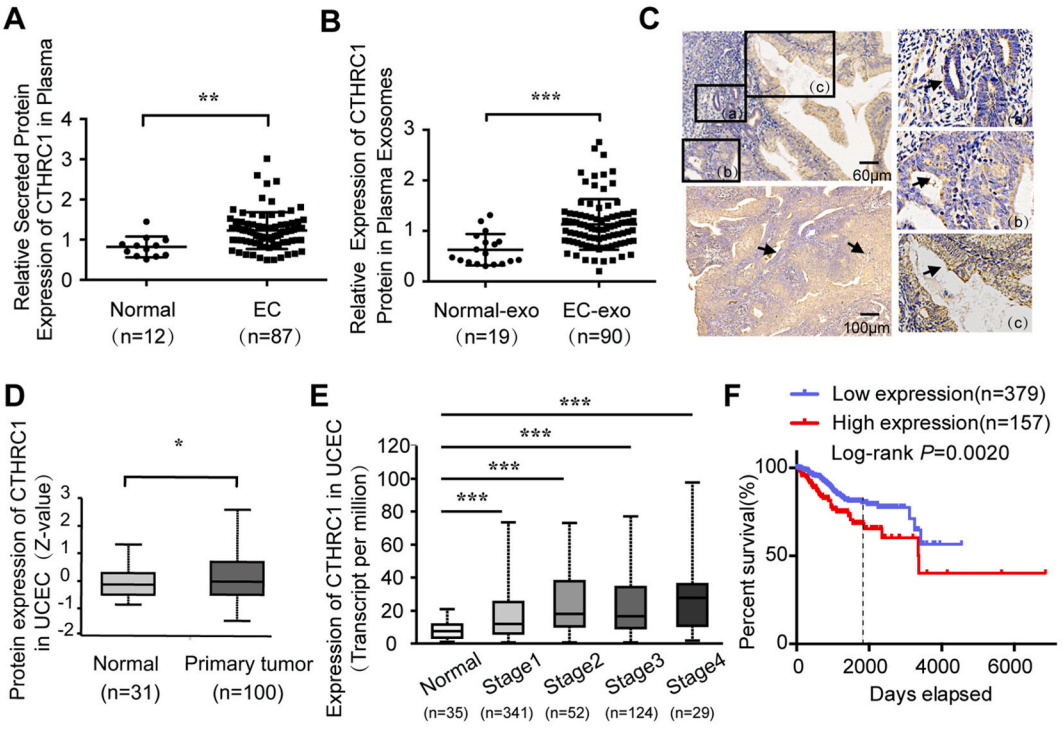

Fig. 5. CTHRC1 expression in EC was correlated with cancer progression and prognosis A ELISA analysis of secreted CTHRC1 levels in plasma of normal females or EC patients (normal group, n = 12; EC group, n = 39; **$P < 0.01$). B Protein levels of exosomal CTHRC1 in plasma of normal females or EC patients (normal group, n = 19; EC group, n = 90; ***$P < 0.001$). **C** Immunohistochemical analysis of CTHRC1 expression in normal endometrium (a), atypical proliferative endometrium (b), and endometrial cancer tissue (c). **D** The protein levels analysis in uterine corpus endometrial carcinoma database derived from CPTAC and ICPC datasets (*$P < 0.05$). **E** CTHRC1 expression levels in EC at different stages with TCGA data (***$P < 0.001$). **F** Kaplan–Meier curve and log-rank test were performed to analyze effect of CTHRC1 expression level on the overall survival of EC patients (low CTHRC1 expression, n = 379; high CTHRC1 expression, n = 157; $P = 0.0020$).

2.2. CAF-derived exosomes increased proliferation and migration of EC cells in vitro

Having demonstrated that culture media of CAFs could increase cell proliferation and migration, we next assessed CAFs derived exosomes could also elicit this change. We isolated exosomes from cell culture media collected from NFs and CAFs using ultracentrifugation. Transmission electron microscopy (TEM) was applied to visualize spherical exosomes encapsulated by the double-layer membrane (Fig. 2A) and nanoparticle tracking analysis (NTA) showed that exosomes have a typical size ranging from 30 to 150 nm (Fig. 2B). Western blot analysis subsequently confirmed the expression of exosomal markers HSP70, CD63 and CD81 (Fig. 2C). In addition, we evaluated uptake of NF/CAF-derived exosomes by EC cells using fluorescent dye Dil. Ishikawa or AN3CA cells were cultured with Dil-labeled exosomes for 16 h and internalized and accumulated red fluorescence around the nucleus in Ishikawa and AN3CA cells indicated efficient exosome uptake (Fig. 2D).

Furthermore, we examined the impact of exosomes derived from NFs and CAFs on the behavior of recipient EC cells. As illustrated in Fig. 2E, CAF-derived exosomes (n = 5) were found to significantly boost the proliferation of Ishikawa cells at an exosome concentration of 100 μg/ml and AN3CA cells at 25, 50 or 100 μg/ml, in comparison to NF-derived exosomes (n = 5) or negative control. For migration, NF-derived exosomes effectively reduced migrated cells in transwell assay, whereas the cell migration capacity of EC cells significantly improved after incubation with CAF-derived exosomes (Fig. 2F). These results indicated that exosomes derived from CAFs were positively involved in EC progression.

2.3. Identification of oncogenic protein CTHRC1 in CAF-derived exosomes

To explore ubiquitous and abundant exosomal proteins, we exploited tandem mass tag (TMT) labeled quantitative proteomics of exosomes secreted by NFs and CAFs (n = 5 per group). A total of 673 proteins were identified and 623 proteins were quantified in different groups. Based on protein information following crude screening, fold change (FC) FC > 1.5 or FC < 2/3 and P-value <0.05 were used as criteria for selecting upregulated or downregulated proteins. Eventually, 17 upregulated proteins and 52 downregulated proteins were screened as proteins differently expressed between NFs and CAFs derived exosomes, as depicted in a volcano plot (Fig. 3A). Furthermore, A heatmap showed 17 upregulated proteins and 13 downregulated proteins (NFs vs. CAFs-exo, FC > 1.5 or FC < 0.5; Fig. 2B). Analysis of the KEGG pathway showed that upregulated proteins were enriched in extracellular matrix (ECM)-receptor interaction, focal adhesion, and PI3K-AKT signaling transduction (Fig. 3C). Among the proteins under consideration, extensive research was conducted on the protein CTHRC1, which had been shown to be associated with cancer progression, and CTHRC1 expression was elevated in CAF-exo when compared to NF-exo (Fig. 3D). Western blotting was conducted to confirm proteomic analysis of different expressions of CTHRC1 in exosomes derived from NFs and CAFs (Fig. 3E). Intriguingly, the variance in RNA and protein levels of CTHRC between NFs and CAFs did not display statistical significance (Fig. 3F and G).

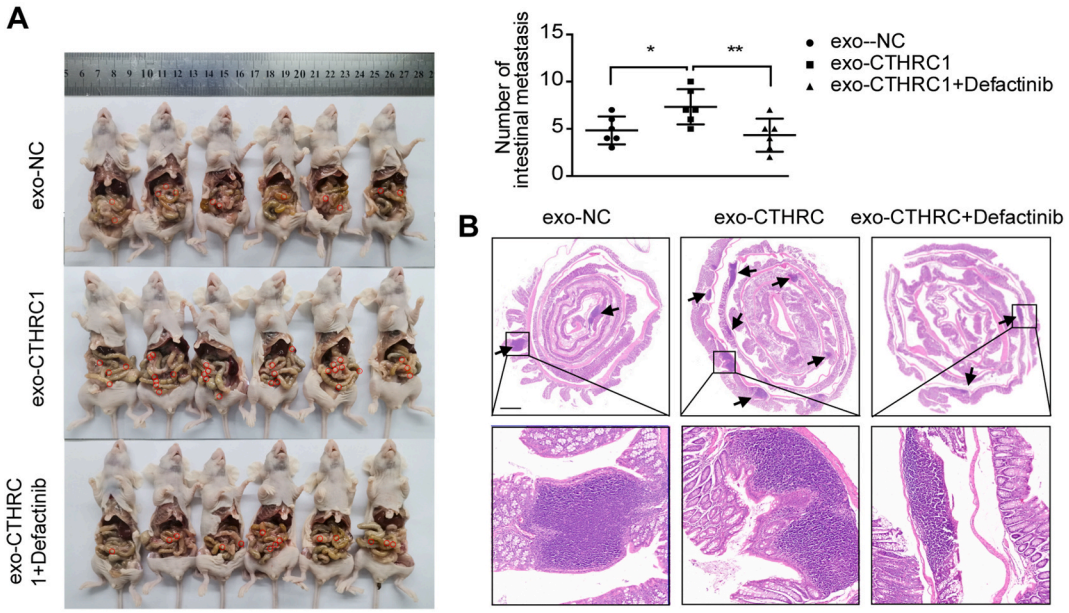

Fig. 6. The involvement of exosomal CTHRC1 in the intestinal metastasis of EC. A,B Number of tumor nodes after treatment with PBS, exosomes or exosomes and Defactinib in intraperitoneal transplanted mouse model (n = 6 per group; exo-NC vs exo-CTHRC1, *$P < 0.05$; exo-CTHRC1 vs exo-CTHRC1+Defactinib, *$P < 0.01$).

2.4. Abundant CTHRC1-loaded exosomes contribute to EC cell migration by activating the ITGB3/FAK signaling pathway

To explore the function and mechanism of exosomal CTHRC1 in EC progression, we generated exosomes with high levels of CTHRC1 protein by overexpressing CTHRC1 in human embryonic kidney 293 (HEK293) cells. Western blot analysis confirmed CTHRC1 was efficiently overexpressed in HEK293 cells (Fig. 4A). CTHRC1-enriched exosomes (exo-CTHRC1) and control group exosomes (exo-NC) were collected from HEK293 cell culture medium by ultracentrifugation. Expression of exosomal CTHRC1 and specific exosomal markers (HSP70, CD63 and CD81) were determined by western blotting (Fig. 4A). Morphology and particle size distribution of exosomes were observed using TEM and NTA (Fig. 4C and D). After incubation for 16 h, it was confirmed that both exo-NC and exo-CTHRC1 were taken up by nearly all Ishikawa and AN3CA cells (Fig. 4E). Cell Counting Kit-8 revealed that there was no significant alteration in cell proliferation following treatment with CTHRC1-enriched exosomes (Fig. 4F). However, exo-CTHRC1 effectively enhanced the migration of Ishikawa and AN3CA cells (Fig. 4G).

To elucidate plausible mechanisms underlying the enhancement of EC progression by CTHRC1, we examined the ITGB3/FAK signaling pathway. Western blotting showed elevated expression of ITGB3 and phosphorylated FAK (at Thy397) after exposure to exo-CTHRC1 in comparison to exo-NC treatment (Fig. 4H). To further identify the relationship between CTHRC1 and ITGB3, co-immunoprecipitation for CTHRC1 and ITGB3 in EC cells revealed that the ITGB3 was immunoprecipitated by CTHRC1 antibody (Fig. 4I). Meanwhile, we verified the effect of FAK signaling on exo-CTHRC1 triggered migration utilizing Defactinib, an inhibitor of FAK Tyr397 phosphorylation. The addition of Defactinib restrained exo-CTHRC1 induced expression of P-FAK (Tyr397) and abolished the migration capacities of Ishikawa and AN3CA cells (Fig. 4J and K). The findings indicated that exo-CTHRC1 physically interacted with ITGB3, leading to an increase in ITGB3 expression and subsequent activation of FAK phosphorylation at Tyr397 to promote the migration of EC cells.

2.5. CTHRC1 expression in EC was correlated with cancer progression and prognosis

Considering CTHRC1 as a secreted protein, in order to comprehensively understand its function in endometrial cancer, we studied the expression levels of both secreted CTHRC1 and exosomal CTHRC1 in the plasma of EC patients. The level of secreted CTHRC1 in plasma was increased in EC patients when compared with healthy individuals (Fig. 5A). Additionally, elevated plasma exosomal CTHRC1 levels were also observed in EC patients (Fig. 5B). Moreover, immunohistochemistry staining of EC tissue indicated that CTHRC1 expression levels were upregulated in tandem with tumor progression. As illustrated in Fig. 5C, expression of CTHRC1 gradually increased in normal endometrium (a), atypical proliferative endometrium (b), and endometrial cancer tissue (c). Furthermore, CTHRC1 was not only highly expressed in glandular epithelial tissue, but also strongly stained in stromal tissue. Subsequently, we analyzed the protein levels in uterine corpus endometrial carcinoma database derived from Clinical Proteomic Tumor Analysis Consortium (CPTAC) and the International Cancer Proteogenome Consortium (ICPC) datasets using UALCAN (http://ualcan.path.uab.edu). CTHRC1 exhibited high expression levels in EC tissue compared to that of normal tissue, and the transcription levels increased progressively during tumor progression (Fig. 5E). Analysis of the TCGA database revealed a correlation between high levels of CTHRC1 expression and poor overall survival in EC patients (Fig. 5F).

2.6. Exosomal CTHRC1 promote intraperitoneal metastasis of EC in vivo

To further evaluate the impact of exo-CTHRC1 on EC metastasis *in vivo*, we created a mouse model of EC metastasis with intraperitoneal injection (n = 6 mice per group). As displayed in Fig. 6, exo-CTHRC1 significantly boosted intestinal metastasis of EC. In addition, intraperitoneal injection of Defactinib abolished exo-CTHRC1-induced metastasis of EC in mouse models, demonstrating the significance of FAK phosphorylation in this process.

3. Discussion

TME, a complex and constantly evolving entity, orchestrated by intercellular communication, is responsible for cancer progression and metastasis. Therefore, uncovering the regulatory mechanisms between cancer and stromal cells mediated by exosomes is critical to developing an anti-tumor strategy. In EC, exosomes containing lncRNA NEAT1 from CAFs were reported to contribute to endometrial cancer progression via miR-26a/b-5p-mediated STAT3/YKL-40 pathway [19]. Direct transfer of CAF-derived exosomal miR-320a to EC cells has been demonstrated to inhibit proliferation by downregulating HIF1alpha, resulting in reduced VEGFA expression *in vitro* [20]. It has also been shown that downregulated miR-148b in exosomes secreted by CAFs induced epithelial-mesenchymal transition of endometrial cancer cells [21]. In this study, we performed proteomic analysis for the first time and the results showed that the level of CTHRC1 in exosomes released from CAFs was increased in EC. In addition, we demonstrated that exosomal CTHRC1 improved migration of EC cells in an ITGB3/FAK-dependent manner *in vitro*, boosting the number of metastatic tumors in the mouse peritoneal metastasis model of endometrial cancer. Moreover, we found that circulating exosomal CTHRC1 was elevated in EC plasma, correlated with tumor progression and poor prognosis.

Collagen triple helix repeat containing-1 (CTHRC1), was highly conserved from lower chordates to mammals and was initially identified as a differentially expressed gene in balloon-injured rat arteries compared to normal ones [22]. As a secreted protein, CTHRC1 interacts with various intracellular and extracellular matrices in complex ways. It has been found that CTHRC1 is significantly upregulated at both mRNA and protein levels in multiple tumors compared to adjacent normal tissues. CTHRC1 is involved in tumorigenesis and development, including tumor cell motility, proliferation, invasion, metastasis of tumor lymph nodes, and patient

prognosis [23–26]. In this study, we found that exosomal CTHRC1, as well as secreted CTHRC1, was significantly increased in plasma of EC patients, suggesting an alternative mechanism for CTHRC1 to promote tumor progression. Encapsulation by exosomes enables CTHRC1 to exert its effects not only through paracrine signaling on nearby tumor cells, but also remotely through fluid transport, promoting the formation of a pre-metastatic microenvironment and facilitating tumor metastasis.

Studies have shown that that CTHRC1 exerts its effects through several signaling pathways such as the TGF-β, Wnt, integrin β/FAK, Src/FAK, MEK/ERK, PI3K/AKT/ERK, HIF-1α, and PKC-δ/ERK signaling pathways [27]. Integrins are transmembrane receptors that facilitate cell interaction with the extracellular matrix. Comprising two distinct subtypes, α and β, they play a critical role in numerous physiological processes, including tumor progression and cell migration [28]. Integrins are recognized as the primary regulators of FAK [29]. Previous researches have demonstrated that targeting the integrin β3 (ITGB3)/FAK signaling pathway could enhance the antitumor activity and attenuate cancer metastasis, such as melanoma, ovarian cancer, and endometrial cancer [30–32]. Focal adhesion kinase (FAK) is a non-receptor tyrosine kinase, involved in numerous cellular operations. Upon stimulation, FAK auto-phosphorylates at Tyr397, Tyr567, and Tyr577, triggering tumorigenesis, epithelial plasticity, metastatic reactivation, and resistance to oncogene- and immune-directed therapies [33]. Defactinib is a highly effective second-generation FAK inhibitor, inhibiting FAK-Y397 phosphorylation in a time- and dose-dependent manner in cancer cells [34]. Despite its limited efficacy as a monotherapy for cancer, defactinib effectively synergizes with other agents, potentially reversing therapeutic failures and enhancing the effectiveness of immunotherapeutic strategies against solid tumors [35,36]. Conformably, our research implicated that CAF-derived exosomal CTHRC1 interacted with ITGB3 physically, upregulating its expression and activating the phosphorylation of FAK at Tyr-397. However, further experiments are needed to clarify the mechanisms behind CTHRC1 overexpression, secretion, and packaging into exosomes within CAF cells.

Recent advances in CAF molecular and functional heterogeneity open new avenues for cancer treatment. Targeting CAF-secreted immunosuppressive and tumor-promoting ligands like IL-6, LIF, and TGF-β could prove to be potential strategies for cancer treatment [37–39]. Compared to solid tumors of other organ types, the uterine endometrium contains a high amount of fibroblast-rich stroma surrounding the glandular epithelium. Although cross-talk between CAFs and tumor cells has been studied in other solid tumors [40, 41], its functional relevance and impact on EC progression is not fully understood. Although our study found that CAFs had increased expression of CTHRC1 with neoplasia, it remains uncertain whether elevated expression of CTHRC1 is a driving force for tumor progression or a result of tumor cell activity. The ongoing revolution in single-cell omics, with single-cell RNA sequencing leading the way, providing novel and important insights into TME, the highly complex and dynamic biological systems, helping to reveal dynamic crosstalk between CAF and tumor cells in time and space [42–44].

To conclude, it was found that the expression of CTHRC1 was higher in exosomes originating from CAFs when compared to those derived from NFs. Exosomal CTHRC1 present in ECM was transferred to EC cells, activating the ITGB3/FAK signaling pathway, and promoting the tumor progression. This research highlights the vital role of CAF-derived exosomes in the development of EC. Further investigations are necessary to identify potential therapeutic strategies for future intervention.

4. Materials and methods

4.1. Experimental ethics statement

All studies involving human materials and animal studies were granted ethical approval by the Ethics Committee of Shanghai First Maternity and Infant Hospital, Tongji University School of Medicine (approval document No. KS20132). Written consents were signed by the participants for the use of tissue for comprehensive experiments.

4.2. Primary cell isolation and general cell line culture

Primary normal fibroblasts (NFs) and cancer-associated fibroblasts (CAFs) were isolated from normal endometrial tissue and endometrial cancer tissue separately. Briefly, tissue samples were sampled by pathologists after surgery immediately, minced into small fragments, trypsinized with Collagenase I (Sigma-Aldrich, Shanghai, China) for 4 h at 37 °C in agitation and filtrated though a 70-μm pore filter to remove undigested tissue. After filtration through a 40-μm pore filter, the single-cell suspension was centrifugated to collect primary fibroblast. Human EC cell lines (Ishikawa and AN3CA) and HEK293 cells from the American Type Culture Collection (ATCC) were tested negative for mycoplasma. EC cells and HEK293 cells were cultured in Dulbecco's Modified Eagle's Medium (DMEM)/F12 medium (HyClone, Chicago, USA) and high-glucose DMEM (HyClone, Chicago, USA) separately, supplemented with 10 % FBS(Gibco, CA, USA) and 1 % PenStrep (100 U/ml penicillin&100 μg/ml streptomycin, Gibco, CA, USA) at 37 °C in humidified 5 % CO2 atmosphere.

4.3. Immunofluorescence (IF)

Cells were seeded in 6 cm dish for confocal microscopy and fixed with 4 % paraformaldehyde at room temperature for 15 min. Following a wash with PBS, cells were permeabilized with 0.5 % Triton X-100 for 15 min, blocked with 2 % bovine serum albumin (BSA, Sigma-Aldrich, Shanghai, China) for 15 min, incubated with primary antibodies at 4 °C overnight, followed by incubation with fluorescence-labeled secondary antibodies for 1 h in the dark. Cell nuclei were stained with DAPI (Sigma, Darmstadt, Germany) at room temperature for 5 min.

4.4. Exosome isolation

Cells were washed with PBS and cultured with medium containing 10 % exosome-free FBS (Gibco, CA, USA) for 48 h. Then medium was collected and subjected to centrifugation at 3,000×*g* for 15 min to remove deceased cells and cellular debris. The supernatant was centrifuged at 10,000×*g* for 60min to eliminate large size vesicles. Exosomes were pelleted by ultracentrifugation at 100,000 g for 120 min. Plasma exosomes were collected using ExoQuick (SBI, CA, USA) following the manufacturer's protocol (https://www.systembio.com/wp/wp-content/uploads/2020/10/MANUAL_EXOQXXA-1-1.pdf). Exosome pellets were resuspended in PBS. All the steps were conducted at a temperature of 4 °C.

Exosome transmission electron microscopy and nanoparticle tracking analysis Exosomes were deposited on a carbon-coated electron microscope grid, fixed with 2 % glutaraldehyde for 5min, stained with uranyl acetate for 2 h, and observed by transmission electron microscopy. The size and distribution of exosomes were determined by ZetaView (Particle Metrix, Meerbusch, Germany).

4.5. Exosome uptake by EC cells

Exosomes were dyed with 1,10-dioctadecyl- 3,3,30,30-tetramethylindocarbocyanine perchlorate (Dil, Thermo Fisher, CA, USA) for 15 min at 37 °C. Cells were incubated with Dil-labeled exosomes for 16 h, fixed in 4 % paraformaldehyde for 10 min, permeabilized with 0.5 % Triton X-100 for 15 min, blocked with 1 % BSA (Sigma-Aldrich) for 15 min and dyed with phalloidin-FITC (Sigma, Darmstadt, Germany) and DAPI (Sigma). Images were captured using confocal microscopy (TCS SP8; Leica, Wentzler, Germany).

4.6. Exosome quantitative proteomics analysis

Total protein tandem mass tag (TMT) labeling, high-performance liquid chromatography (HPLC) classification technology and quantitative proteomics technology based on mass spectrometry were utilized to analyze purified proteins from exosome samples. Briefly, exosome protein concentration was determined by Pierce BCA protein assay kit (Thermo Fisher Scientific). Peptides were desalted with Strata X C18 (Phenomenex), vacuum-dried, and reconstituted in 0.5 M TEAB and processed according to the manufacturer's protocol for TMT kit kit after trypsin digestion. Tryptic peptides were fractionated by high pH reverse-phase HPLC using Agilent 300Extend C18 column (5 μm particles, 4.6 mm ID, 250 mm length), dissolved in 0.1 % formic acid, loaded onto an EASY-nLC 1000 UPLC system (15 cm length, 75 μm i.d.), subjected to NSI source and followed by tandem mass spectrometry (MS/MS) in Q ExactiveTM Plus (Thermo) coupled online to the UPLC. Data were processed using the Maxquant search engine (v.1.5.2.8).

4.7. Lentiviral transduction in HEK293 cells

Human CTHRC1 (NM_138455) cDNA was cloned into a lentiviral vector containing CMV-MCS-PGK-Puro (Hanyin Biotechnology, Shanghai, China). Puromycin (1 μg/ml) was used to select stable transfected HEK293 cell clones (overexpressing CTHRC1 or the negative control) after 48 h of lentiviral transduction. CTHRC1-overexpressing or negative control exosomes (exo-CTHRC1 or exo-NC) were purified from cell culture medium.

4.8. Cell proliferation

EC cells were seeded in 96-well plates (2,500 cells per well) for 16 h. Different concentrations of exosomes were incubated with cells for 72 h. 10 μl of cell counting kit-8 (MCE, Shanghai, China) was added to each well and incubated at 37 °C for 1 h. Absorption was measured at 450 nm using a microplate spectrophotometer.

4.9. Cell migration

Ishikawa (60,000 cells) and AN3CA (30,000 cells) were resuspended in 100 μl serum-free medium and seeded into the upper transwell chambers (8 μm pore size, No.3422, Corning Costar). The bottom chamber (24-well plates) was filled with 400 μl of 20 % exosome-free FBS serving as a chemoattractant. 100 μl and 400 μl exosomes (200 μg/ml) in serum-free medium were added to upper and bottom chambers respectively, ensuring a final exosome concentration of 100 μg/ml on both sides. After incubating for 16 h, migrated cells were stained with 0.2 μg/ml calcein AM (No. C3100MP, Invitrogen Life Technologies) for 30min and imaged by fluorescence microscope (Nikon, Tokyo, Japan).

4.10. RNA extraction and qRT-PCR

Total RNA was purified with Trizol (Invitrogen, CA, USA) and converted into cDNA with One Step PrimeScript RT reagent kit with gDNA Eraser (#RR047A, Takara, Japan) following the manufacturer's directions. The primers were synthesized by Sangon Biotech (Shanghai, China). Quantitative real-time PCR (qRT-PCR) analyses were performed on ABI Prism 7000 thermal cycler (Applied Biosystems) using SYBR Premix Ex Taq II (#RR820A, Takara, Japan). Gene expression was calculated using the 2-ΔΔCt formula.

4.11. Protein extraction and Western blot analysis

Protein was lysed by RIPA buffer (Beyotime Biotechnology, Shanghai, China). Equal amounts of protein were loaded onto each lane of a SDS-PAGE gel for protein separation and transferred to polyvinylidene fluoride membranes (PVDF, Millipore, Billerica, MA, USA). The membranes were blocked with 5 % bovine serum albumin for 2 h and incubated with antibodies against exosome-specific markers (CD9, CD63, and CD81; 1:1000, EXOAB-KIT-1, SBI, CA, USA), FAP (1:1000, ab53066, Abcam), α-SMA (1:1000, #19245, Cell Signalling Technology (CST), Chicago, USA), GAPDH (1:1000, #8884, CST), CTHRC1 (1 mg/ml, ab85739, Abcam), ITGB3 (1:1000, #13166, CST), *p*-FAK (1:1000, #8556, CST), and FAK (1:1000, #3285, CST) overnight at 4 °C, followed by incubation with HRP-conjugated secondary antibodies (1:2000, #7074,CST) for 2 h at room temperature. Blotted proteins were visualized using an enhanced chemiluminescence kit (Millipore, Burlington, MA) and imaged using a FluorChem E imaging instrument (Tanon, China).

4.12. Elisa assay

CTHRC1 levels in human plasma and plasma exosomes were determined using an ELISA kit from SAB (#13502Jiangsu, China) following manual instruction.

4.13. Co-IP

After treatment with exo-CTHRC1, cell lysates pretreated using Protein A/G Sepharose beads (Sigma, Germany) were incubated with CTHRC1 antibody (Proteintech, 16534-1-AP) and IgG as control at 4 °C overnight. The beads were washed by PBS containing 1 % PMSF three times, mixed with loading buffer and incubated at 100 °C for 10 min. After centrifugation at 10,000 g for 4 min, the supernatants were analyzed by Western blot.

4.14. CTHRC1 expression in database and Kaplan-Meier survival analysis of EC patients

The bioinformatics portal UALCAN (http://ualcan.path.uab.edu) was used to analyze the expression of CTHRC1 in Clinical Proteomic Tumor Analysis Consortium (CPTAC) and the International Cancer Proteogenome Consortium (ICPC) uterine corpus endometrial carcinoma database [45,46]. Data for expression of CTHRC1 mRNA in EC patients were obtained from the OncoLnc database (http://www. oncolnc.org) [47]. The optimal cut-off point for CTHRC1 level was calculated by the X-tile program and the prognostic value for EC patients was examined using Kaplan-Meier survival analysis.

4.15. Animal tumor metastasis model

Female nude mice (4–5 weeks) were obtained from the Hubei Laboratory Animal Centre of Tongji University (Shanghai, China) and randomly divided into three groups (n = 6) for intraperitoneal injection with 2 × 105 (100 μL) AN3CA cells. Exo-CTHRC1 (10 mg/kg) alone or in combination with Defactinib (25 mg/kg, HY-12289, MedChemExpress, Shanghai, China) were injected intraperitoneally every five days, exo-NC was used as a negative control. Animals were cared for according to standard protocols for laboratory animals. Thirty days after the initial injection, the intestines of the mice were harvested following euthanasia. The tissues were fixed using formalin solution, processed into Swiss Roll form, embedded in paraffin, stained with Hematoxylin-Eosin (HE), and subjected to immunohistochemical analysis for histological examination.

4.16. Statistical analyses

All data are presented as the means ± SEM deviation. Data generated displayed normal distribution with similar variances, and analysis was performed assuming equal variances. For nonparametric data, the Kruskal–Wallis H test was performed. Statistical significance was calculated with GraphPad Prism software using a Student *t*-test (one-sided) or ANOVA as appropriate. *P < 0.05, **P < 0.01, ***P < 0.001.

Data availability statement

Upon reasonable inquiry, all supporting data and methods for this study will be provided by its corresponding author.

CRediT authorship contribution statement

Yiding Bian: Writing – original draft, Visualization, Funding acquisition, Data curation. **Xinwen Chang:** Methodology, Investigation. **Xiang Hu:** Validation. **Bilan Li:** Resources, Funding acquisition. **Yunfeng Song:** Validation, Software. **Zhiyi Hu:** Formal analysis. **Kai Wang:** Project administration, Methodology, Conceptualization. **Xiaoping Wan:** Writing – review & editing, Resources, Methodology. **Wen Lu:** Writing – review & editing, Supervision.

Declaration of competing interest

The authors declare the following financial interests/personal relationships which may be considered as potential competing interests:Bian Yiding reports financial support was provided by National Natural Science Foundation of China. Wan Xiaoping reports financial support was provided by Natural Science Foundation of Shanghai. If there are other authors, they declare that they have no known competing financial interests or personal relationships that could have appeared to influence the work reported in this paper.

Acknowledgements

This study was sponsored by National Natural Science Foundation of China (grant numbers 87002723, 82172714, 81602281, and 81971338), Natural Science Foundation of Shanghai (grant numbers 2Y11906300 and 20ZR1443900), Clinical Research Plan of SHDC (grant numbers SHDC2020CR4086, SHDC2020CR5003-002, and SHDC12020107).

References

[1] H. Sung, J. Ferlay, R.L. Siegel, et al., Global cancer statistics 2020: GLOBOCAN estimates of incidence and mortality worldwide for 36 cancers in 185 countries, CA A Cancer J. Clin. 71 (3) (2021) 209–249, https://doi.org/10.3322/caac.21660.
[2] R.L. Siegel, K.D. Miller, A. Jemal, Cancer statistics, 2018, CA A Cancer J. Clin. 68 (1) (2018) 7–30, https://doi.org/10.3322/caac.21442.
[3] H.O. Sai Varshith, J. Vaidya, S. Sural, V. Atluri, Enabling attribute-based access control in Linux Kernel, Asia CCS 22 (2022) 1237–1239, https://doi.org/10.1145/3488932.3527293, 2022;2022.
[4] H. Zhang, X. Yue, Z. Chen, et al., Define cancer-associated fibroblasts (CAFs) in the tumor microenvironment: new opportunities in cancer immunotherapy and advances in clinical trials, Mol. Cancer 22 (1) (2023) 159, https://doi.org/10.1186/s12943-023-01860-5. Published 2023 Oct 2.
[5] N.A. Giraldo, R. Sanchez-Salas, J.D. Peske, et al., The clinical role of the TME in solid cancer, Br. J. Cancer 120 (1) (2019) 45–53, https://doi.org/10.1038/s41416-018-0327-z.
[6] R. Baghban, L. Roshangar, R. Jahanban-Esfahlan, et al., Tumor microenvironment complexity and therapeutic implications at a glance, Cell Commun. Signal. 18 (1) (2020) 59, https://doi.org/10.1186/s12964-020-0530-4. Published 2020 Apr 7.
[7] N.M. Anderson, M.C. Simon, The tumor microenvironment, Curr. Biol. 30 (16) (2020) R921–R925, https://doi.org/10.1016/j.cub.2020.06.081.
[8] K.S. Subramaniam, I.S. Omar, S.C. Kwong, et al., Cancer-associated fibroblasts promote endometrial cancer growth via activation of interleukin-6/STAT-3/c-Myc pathway, Am. J. Cancer Res. 6 (2) (2016) 200–213. Published 2016 Jan 15.
[9] X. Wang, W. Zhang, X. Sun, Y. Lin, W. Chen, Cancer-associated fibroblasts induce epithelial-mesenchymal transition through secreted cytokines in endometrial cancer cells, Oncol. Lett. 15 (4) (2018) 5694–5702, https://doi.org/10.3892/ol.2018.8000.
[10] F. Teng, W.Y. Tian, Y.M. Wang, et al., Cancer-associated fibroblasts promote the progression of endometrial cancer via the SDF-1/CXCR4 axis, J. Hematol. Oncol. 9 (2016) 8, https://doi.org/10.1186/s13045-015-0231-4. Published 2016 Feb 6.
[11] S. Mochizuki, T. Ao, T. Sugiura, et al., Expression and function of a disintegrin and metalloproteinases in cancer-associated fibroblasts of colorectal cancer, Digestion 101 (1) (2020) 18–24, https://doi.org/10.1159/000504087.
[12] O. Aprelikova, J. Palla, B. Hibler, et al., Silencing of miR-148a in cancer-associated fibroblasts results in WNT10B-mediated stimulation of tumor cell motility, Oncogene 32 (27) (2013) 3246–3253, https://doi.org/10.1038/onc.2012.351.
[13] T. Inoue, K. Adachi, K. Kawana, et al., Cancer-associated fibroblast suppresses killing activity of natural killer cells through downregulation of poliovirus receptor (PVR/CD155), a ligand of activating NK receptor, Int. J. Oncol. 49 (4) (2016) 1297–1304, https://doi.org/10.3892/ijo.2016.3631.
[14] L. Jiang, Y. Gu, Y. Du, J. Liu, Exosomes: diagnostic biomarkers and therapeutic delivery vehicles for cancer, Mol. Pharm. 16 (8) (2019) 3333–3349, https://doi.org/10.1021/acs.molpharmaceut.9b00409.
[15] M. Osaki, F. Okada, Exosomes and their role in cancer progression, Yonago Acta Med. 62 (2) (2019) 182–190, https://doi.org/10.33160/yam.2019.06.002. Published 2019 Jun 20.
[16] D.K. Jeppesen, Q. Zhang, J.L. Franklin, R.J. Coffey, Extracellular vesicles and nanoparticles: emerging complexities, Trends Cell Biol. 33 (8) (2023) 667–681, https://doi.org/10.1016/j.tcb.2023.01.002.
[17] Q.F. Han, W.J. Li, K.S. Hu, et al., Exosome biogenesis: machinery, regulation, and therapeutic implications in cancer, Mol. Cancer 21 (1) (2022) 207, https://doi.org/10.1186/s12943-022-01671-0. Published 2022 Nov 1.
[18] R. Isaac, F.C.G. Reis, W. Ying, J.M. Olefsky, Exosomes as mediators of intercellular crosstalk in metabolism, Cell Metabol. 33 (9) (2021) 1744–1762, https://doi.org/10.1016/j.cmet.2021.08.006.
[19] J.T. Fan, Z.Y. Zhou, Y.L. Luo, et al., Exosomal lncRNA NEAT1 from cancer-associated fibroblasts facilitates endometrial cancer progression via miR-26a/b-5p-mediated STAT3/YKL-40 signaling pathway, Neoplasia 23 (7) (2021) 692–703, https://doi.org/10.1016/j.neo.2021.05.004.
[20] N. Zhang, Y. Wang, H. Liu, W. Shen, Extracellular vesicle encapsulated microRNA-320a inhibits endometrial cancer by suppression of the HIF1α/VEGFA axis, Exp. Cell Res. 394 (2) (2020) 112113, https://doi.org/10.1016/j.yexcr.2020.112113.
[21] B.L. Li, W. Lu, J.J. Qu, L. Ye, G.Q. Du, X.P. Wan, Loss of exosomal miR-148b from cancer-associated fibroblasts promotes endometrial cancer cell invasion and cancer metastasis, J. Cell. Physiol. 234 (3) (2019) 2943–2953, https://doi.org/10.1002/jcp.27111.
[22] P. Pyagay, M. Heroult, Q. Wang, et al., Collagen triple helix repeat containing 1, a novel secreted protein in injured and diseased arteries, inhibits collagen expression and promotes cell migration, Circ. Res. 96 (2) (2005) 261–268, https://doi.org/10.1161/01.RES.0000154262.07264.12.
[23] W. He, H. Zhang, Y. Wang, et al., CTHRC1 induces non-small cell lung cancer (NSCLC) invasion through upregulating MMP-7/MMP-9, BMC Cancer 18 (1) (2018) 400, https://doi.org/10.1186/s12885-018-4317-6. Published 2018 Apr 10.
[24] X.L. Zhang, L.P. Hu, Q. Yang, et al., CTHRC1 promotes liver metastasis by reshaping infiltrated macrophages through physical interactions with TGF-β receptors in colorectal cancer, Oncogene 40 (23) (2021) 3959–3973, https://doi.org/10.1038/s41388-021-01827-0.
[25] X.F. Jin, H. Li, S. Zong, H.Y. Li, Knockdown of collagen triple helix repeat containing-1 inhibits the proliferation and epithelial-to-mesenchymal transition in renal cell carcinoma cells, Oncol. Res. 24 (6) (2016) 477–485, https://doi.org/10.3727/096504016X14685034103716.
[26] D. Peng, C. Wei, X. Zhang, et al., Pan-cancer analysis combined with experiments predicts CTHRC1 as a therapeutic target for human cancers, Cancer Cell Int. 21 (1) (2021) 566, https://doi.org/10.1186/s12935-021-02266-3. Published 2021 Oct 26.
[27] D. Mei, Y. Zhu, L. Zhang, W. Wei, The role of CTHRC1 in regulation of multiple signaling and tumor progression and metastasis, Mediat. Inflamm. 2020 (2020) 9578701, https://doi.org/10.1155/2020/9578701. Published 2020 Aug 12.
[28] Y.L. Chen, T.H. Wang, H.C. Hsu, R.H. Yuan, Y.M. Jeng, Overexpression of CTHRC1 in hepatocellular carcinoma promotes tumor invasion and predicts poor prognosis, PLoS One 8 (7) (2013) e70324, https://doi.org/10.1371/journal.pone.0070324. Published 2013 Jul 29.
[29] S.K. Mitra, D.D. Schlaepfer, Integrin-regulated FAK-Src signaling in normal and cancer cells, Curr. Opin. Cell Biol. 18 (5) (2006) 516–523, https://doi.org/10.1016/j.ceb.2006.08.011.
[30] J. Cooper, F.G. Giancotti, Integrin signaling in cancer: mechanotransduction, stemness, epithelial plasticity, and therapeutic resistance, Cancer Cell 35 (3) (2019) 347–367, https://doi.org/10.1016/j.ccell.2019.01.007.
[31] Y. Kang, W. Hu, C. Ivan, et al., Role of focal adhesion kinase in regulating YB-1-mediated paclitaxel resistance in ovarian cancer, J. Natl. Cancer Inst. 105 (19) (2013) 1485–1495, https://doi.org/10.1093/jnci/djt210.

[32] J.C. Dawson, A. Serrels, D.G. Stupack, D.D. Schlaepfer, M.C. Frame, Targeting FAK in anticancer combination therapies, Nat. Rev. Cancer 21 (5) (2021) 313–324, https://doi.org/10.1038/s41568-021-00340-6.
[33] S.F. Jones, L.L. Siu, J.C. Bendell, et al., A phase I study of VS-6063, a second-generation focal adhesion kinase inhibitor, in patients with advanced solid tumors, Invest. N. Drugs 33 (5) (2015) 1100–1107, https://doi.org/10.1007/s10637-015-0282-y.
[34] C. Luo, J.H. Lim, Y. Lee, et al., A PGC1α-mediated transcriptional axis suppresses melanoma metastasis, Nature 537 (7620) (2016) 422–426, https://doi.org/10.1038/nature19347.
[35] S. Xiong, C. Klausen, J.C. Cheng, H. Zhu, P.C. Leung, Activin B induces human endometrial cancer cell adhesion, migration and invasion by up-regulating integrin β3 via SMAD2/3 signaling, Oncotarget 6 (31) (2015) 31659–31673, https://doi.org/10.18632/oncotarget.5229.
[36] B. Guo, H. Yan, L. Li, K. Yin, F. Ji, S. Zhang, Collagen triple helix repeat containing 1 (CTHRC1) activates Integrin β3/FAK signaling and promotes metastasis in ovarian cancer, J. Ovarian Res. 10 (1) (2017) 69, https://doi.org/10.1186/s13048-017-0358-8. Published 2017 Oct 11.
[37] T.A. Mace, R. Shakya, J.R. Pitarresi, et al., IL-6 and PD-L1 antibody blockade combination therapy reduces tumour progression in murine models of pancreatic cancer, Gut 67 (2) (2018) 320–332, https://doi.org/10.1136/gutjnl-2016-311585.
[38] Y. Shi, W. Gao, N.K. Lytle, et al., Targeting LIF-mediated paracrine interaction for pancreatic cancer therapy and monitoring [published correction appears in Nature. 2021 Dec;600(7889):E18], Nature 569 (7754) (2019) 131–135, https://doi.org/10.1038/s41586-019-1130-6.
[39] D.V.F. Tauriello, S. Palomo-Ponce, D. Stork, et al., TGFβ drives immune evasion in genetically reconstituted colon cancer metastasis, Nature 554 (7693) (2018) 538–543, https://doi.org/10.1038/nature25492.
[40] G. Biffi, D.A. Tuveson, Diversity and biology of cancer-associated fibroblasts, Physiol. Rev. 101 (1) (2021) 147–176, https://doi.org/10.1152/physrev.00048.2019.
[41] L. Monteran, N. Erez, The dark side of fibroblasts: cancer-associated fibroblasts as mediators of immunosuppression in the tumor microenvironment, Front. Immunol. 10 (2019) 1835, https://doi.org/10.3389/fimmu.2019.01835. Published 2019 Aug 2.
[42] V. Bernard, A. Semaan, J. Huang, et al., Single-cell transcriptomics of pancreatic cancer precursors demonstrates epithelial and microenvironmental heterogeneity as an early event in neoplastic progression, Clin. Cancer Res. 25 (7) (2019) 2194–2205, https://doi.org/10.1158/1078-0432.CCR-18-1955.
[43] C.X. Dominguez, S. Müller, S. Keerthivasan, et al., Single-cell RNA sequencing reveals stromal evolution into LRRC15+ myofibroblasts as a determinant of patient response to cancer immunotherapy, Cancer Discov. 10 (2) (2020) 232–253, https://doi.org/10.1158/2159-8290.CD-19-0644.
[44] E. Sahai, I. Astsaturov, E. Cukierman, et al., A framework for advancing our understanding of cancer-associated fibroblasts, Nat. Rev. Cancer 20 (3) (2020) 174–186, https://doi.org/10.1038/s41568-019-0238-1.
[45] D.S. Chandrashekar, B. Bashel, S.A.H. Balasubramanya, et al., UALCAN: a portal for facilitating tumor subgroup gene expression and survival analyses, Neoplasia 19 (8) (2017) 649–658, https://doi.org/10.1016/j.neo.2017.05.002.
[46] D.S. Chandrashekar, S.K. Karthikeyan, P.K. Korla, et al., UALCAN: an update to the integrated cancer data analysis platform, Neoplasia 25 (2022) 18–27, https://doi.org/10.1016/j.neo.2022.01.001.
[47] J. Anaya, OncoLnc: linking TCGA survival data to mRNAs, miRNAs, and lncRNAs, PeerJ Computer Science 2 (2016) e67, https://doi.org/10.7717/peerj-cs.67.